Acta Crystallographica Section D
Biological Crystallography
ISSN 0907-4449

New methods to prepare iodinated derivatives by vaporizing iodine labelling (VIL) and hydrogen peroxide VIL (HYPER-VIL)

Hideyuki Miyatake,[a]* Tomokazu Hasegawa[b] and Akihito Yamano[b]

[a]RIKEN Harima Institute/SPring-8, Koto 1-1-1, Sayo-cho, Sayo-gun, Hyogo 679-5148, Japan, and [b]Rigaku/PharmAxess Inc., 3-9-12 Matsubara-cho, Akishima-shi, Tokyo 196-8666, Japan

Correspondence e-mail: miyatake@postman.riken.jp

New techniques are presented for the preparation of iodine derivatives, involving vapour diffusion of iodine. Firstly, in the vaporizing iodine labelling (VIL) technique, a small amount of KI/I_2 solution is enclosed in a crystallization well, with the result that gaseous I_2 molecules diffuse into the crystallization droplets without exerting substantial changes in ionic strength in the target crystals. Once they have diffused into the droplet, the I_2 molecules sometimes iodinate accessible tyrosines at *ortho* positions. Secondly, when iodination is insufficient, the hydrogen peroxide VIL (HYPER-VIL) technique can be further applied to increase the iodination ratio by the addition of a small droplet of hydrogen peroxide (H_2O_2) to the crystallization well; the gaseous H_2O_2 also diffuses into the crystallization droplet to emphasize the iodination. These techniques are most effective for phase determination when coupled with softer X-rays, such as those from Cu $K\alpha$ or Cr $K\alpha$ radiation. The effectiveness of these techniques was assessed using five different crystals. Four of the crystals were successfully iodinated, providing sufficient phasing power for structure determination.

Received 9 September 2005
Accepted 14 December 2005

PDB References:
VIL-thaumatin, 2d8o, r2d8osf; HYPER-VIL-thaumatin, 2d8p, r2d8psf; HYPER-VIL-trypsin, 2d8w, r2d8wsf; HYPER-VIL-lysozyme, 2d91, r2d91sf; VIL-xylanase, 2dan; VIL′-xylanase, 2d98, r2d98sf.

1. Introduction

Recently, phase determination using softer X-rays ($\lambda > 1.5$ Å) has attracted a considerable degree of attention in the field of protein crystallography (Chayen *et al.*, 2000; Dauter, 2002; Mueller-Dieckmann *et al.*, 2004). The motivation to use softer X-rays has arisen from the success of SAD phasing using only anomalous scattering effects from the sulfurs in native proteins (Dauter *et al.*, 1999). The success of the *de novo* phasing of obelin (Liu *et al.*, 2000) has also contributed to the interest in this technique. Very recently, Kitago *et al.* (2005) reported that their novel method of crystal mounting coupled with the use of Cr $K\alpha$ X-rays successfully enhanced the phasing ability. However, the anomalous effects from sulfur are inherently rather small ($\Delta f'' = 0.56$ e$^-$ at Cu $K\alpha$, 1.5418 Å; $\Delta f'' = 1.14$ e$^-$ at Cr $K\alpha$, 2.2908 Å) compared with those from other conventional heavy atoms and thus the anomalous signals of the S atoms are often insufficient for phase determination in practice.

On the other hand, I atoms diffract softer X-rays with larger anomalous scattering signals, *e.g.* $\Delta f'' = 6.84$ e$^-$ at 1.5418 Å (Cu $K\alpha$ radiation) and $\Delta f'' = 12.14$ e$^-$ at 2.2908 Å (Cr $K\alpha$ radiation). Thus, if we could effectively incorporate iodine into target native crystals, this would greatly improve the chances

Table 1
Basic information about each protein.

Protein	No. of residues (No. of tyrosine residues)	Molecular weight (kDa)	Crystallization conditions
Thaumatin	207 (8)	22.2	0.8 *M* potassium/sodium tartrate, 0.1 *M* Na HEPES pH 7.5
Trypsin	229 (10)	24.0	2.0 *M* ammonium sulfate, 60 m*M* benzamidine, 6 m*M* $CaCl_2$, 50 m*M* Tris–HCl pH 7.5
Lysozyme	129 (3)	14.3	2.0 *M* NaCl, 0.1 *M* sodium acetate, 30%(*v*/*v*) glycerol pH 4.3
Xylanase	176 (17)	19.3	1.5 *M* ammonium sulfate, 0.1 *M* sodium citrate pH 4.3
Glucose isomerase	388 (9)	43.2	2 *M* ammonium sulfate, 0.1 *M* Tris–HCl pH 7.0

of successful phasing using softer X-ray protein crystallography. To date, a variety of methods to derivatize crystals with iodine have been reported. These methods can be categorized into non-genetic and genetic techniques.

Non-genetic preparations of iodine derivatives employ a conventional soaking or short cryosoaking method in which target native crystals are soaked in high-concentration solutions of iodine salts such as KI and NaI or triiodide (Dauter *et al.*, 2000; Nagem *et al.*, 2001, 2005; Dauter, 2002; Evans & Bricogne, 2002, 2003). During the soaking procedures, however, the mosaicities of the target crystals often deteriorate owing to the higher concentration of the iodine-salt solutions. Another approach has been reported in which proteins are crystallized in the presence of NaI or KI (Verdon *et al.*, 2002; Takeda *et al.*, 2004). Although this technique seldom increases the mosaicities, it is only applicable when the iodine salts do not obstruct the crystal growth of the target crystals.

Iodination of tyrosines provides us with another possibility for iodine derivatization, because it produces iodine derivatives with a limited number of highly occupied binding sites. *Ortho*-iodotyrosine with single or double iodination is generated when native crystals are soaked in *N*-iodosuccinamide solution (Brzozowski *et al.*, 1991; Leinala *et al.*, 2002; Zwart *et al.*, 2004). In some cases, soaking of native crystals in triiodide solutions for a longer period (8–60 d) yields *ortho*-iodotyrosine in crystals (Sigler, 1970; Ghosh *et al.*, 1999). To date, however, attempts to prepare *ortho*-iodotyrosine in target crystals have met with only limited success. This is partly because the crystalline order is perturbed by the difference in ionic strength on transferring native crystals to the iodine-compound solution.

Recently, a new genetic method to incorporate *p*-iodophenylalanine (Xie *et al.*, 2004) has been proposed. This technique possesses the virtue of a guaranteed yield of iodinated derivatives, as in the case of the incorporation of selenomethionine into proteins (Hendrickson, 1991). However, these techniques cannot be applied to proteins prepared using non-prokaryotic hosts. Thus, such genetic methods do not satisfy the increasing demand for the structural determination of proteins from natural sources prepared using eukaryotic hosts such as yeasts or insect or animal cells.

In this paper, we present two new techniques, vaporizing iodine labelling (VIL) and hydrogen peroxide VIL (HYPER-VIL), for the preparation of iodinated derivatives involving *ortho*-iodotyrosine residues. The present technique takes advantage of the fact that iodine dissolved in KI solution readily diffuses into the gaseous phase and then into the droplet of mother liquor containing the target crystals, as in the case of derivatization by gaseous xenon or krypton (Schiltz *et al.*, 1994; Stowell *et al.*, 1996; Sauer *et al.*, 1997; Soltis *et al.*, 1997; Owen & Evans, 1998; Cohen *et al.*, 2001; Evans & Bricogne, 2003; Olczak *et al.*, 2003; Mueller-Dieckmann *et al.*, 2004). Thus, the (HYPER)-VIL techniques avoid the serious difference in ionic strength upon derivatization which often causes perturbation of the crystalline order in conventional heavy-atom soaking. The actual procedure of the VIL technique is straightforward. Firstly, a small KI/I_2 droplet is enclosed within a crystallization well that contains the target crystals in a hanging droplet; the gaseous iodine vaporizes and fills the well. The vaporized I_2 molecules gradually diffuse into the hanging droplet and form covalent bonds with tyrosine residues at *ortho* positions by aromatic electrophilic substitution. When the substitution does not occur or is insufficient, the HYPER-VIL technique can be used to enhance the reaction through the addition of a small droplet of hydrogen peroxide to the crystallization well. In HYPER-VIL, gaseous hydrogen peroxide also rapidly diffuses into the droplet, enhancing the substitution reaction. The VIL and HYPER-VIL techniques can be applied to target crystals in a normal atmosphere, requiring no special high-pressure equipment, which is a crucial advantage over the xenon or krypton derivatization.

We applied the presented VIL and/or HYPER-VIL techniques to five test protein crystals: thaumatin, trypsin, lysozyme, xylanase and glucose isomerase. All crystals except glucose isomerase were successfully iodinated. The iodinated derivatives provided sufficient phasing power to build models when in-house Cu $K\alpha$ or Cr $K\alpha$ X-rays coupled with the SAD, SIRAS or MIRAS methods were employed. The presented VIL and HYPER-VIL techniques are useful for permitting phase determination by softer X-ray protein crystallography.

2. Materials and methods

2.1. Preparation of test crystals

Lyophilized protein samples of thaumatin from *Thaumatococcus daniellii*, bovine trypsin and hen-egg white lysozyme were purchased from Sigma (St Louis, MO, USA). Liquid samples of xylanase and glucose isomerase were from Hampton Research (Laguna Niguel, CA, USA). Crystals were prepared by the hanging-drop vapour-diffusion method at 293 K, where 1–2 µl protein solutions were mixed with the same volumes of well solutions, equilibrating against 500 µl of the well solutions in the crystallization wells of 24-well plates (Corning). The sizes of the test proteins and the crystallization conditions are summarized in Table 1.

2.2. Iodine stock solution

To improve the solubility of solid iodine, 250 mg of KI (Wako, Tokyo, Japan) was dissolved in 1 ml H_2O and 135 mg of solid I_2 was then added. The resultant concentration of the iodine stock solution is approximately 0.67 *M* KI and 0.47 *M* I_2 (Evans & Bricogne, 2002). It should be noted that in VIL only I_2 can diffuse in the gaseous phase from the KI/I_2 droplet to the target crystals, although the major iodine components in the stock solution are both I_2 and triiodide (I_3^-). 10 µl samples of the iodine stock solution were stored in small tubes at 243 K. When the iodination experiments were carried out, only the required amount of the frozen iodine stock solution in the tubes was melted at room temperature.

2.3. Iodination of crystals by VIL and/or HYPER-VIL

An example of VIL applied to tetragonal thaumatin crystals is illustrated in Figs. 1(*a*)–1(*d*). Thaumatin crystals were prepared by the hanging-drop vapour-diffusion method (Fig. 1*a*). A small droplet of 0.2 µl KI/I_2 solution was placed beside the crystallization droplet on a cover glass (Fig. 1*b*) and the cover glass was then inverted to form a seal with the crystallization well (Fig. 1*c*), causing the I_2 molecules to rapidly spread throughout the crystallization well and penetrate into the crystallization droplet (Fig. 1*c*). The thaumatin crystals in the droplet soon turned yellowish and then dark brown without any obvious destruction. In this case, the incubation step (Fig. 1*d*) with iodine took 0.5 h at 293 K. The iodination of tyrosines by VIL may proceed according to the chemical reaction shown in Fig. 2.

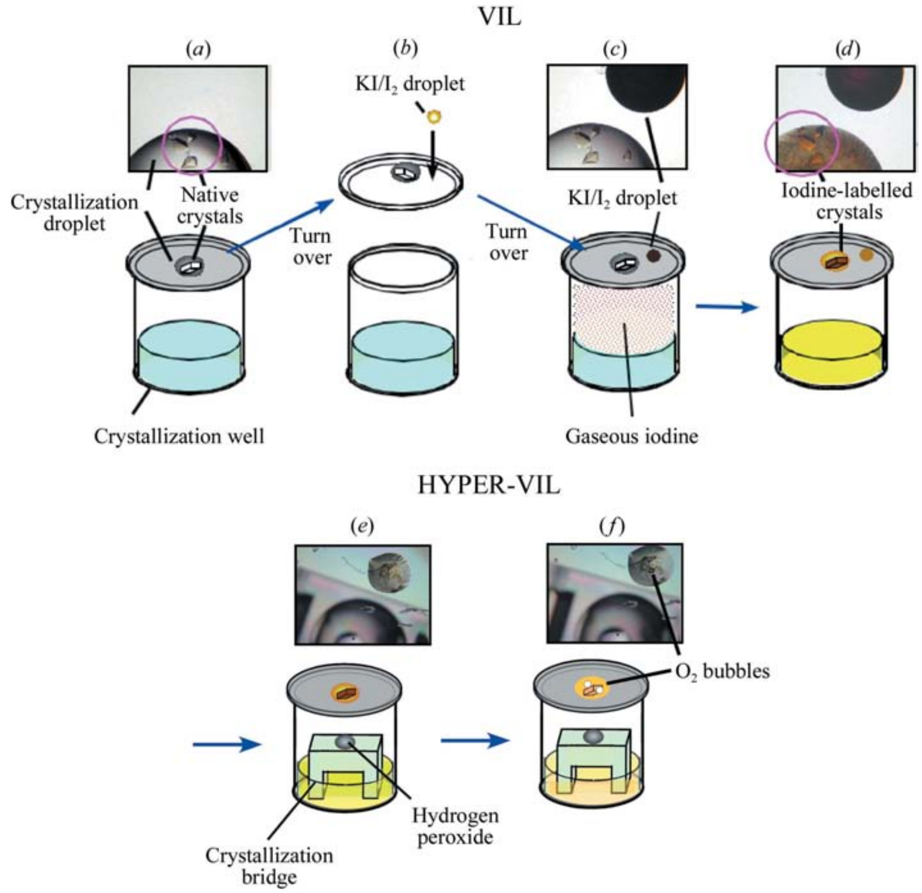

Figure 1
A schematic drawing of VIL (vaporizing iodine labelling) and HYPER-VIL (hydrogen peroxide VIL) procedures applied to representative thaumatin crystals. (*a*) The target native crystals are prepared by the hanging-drop vapour-diffusion method. (*b*) A small droplet of iodine stock solution is placed next to the crystallization droplet on the cover glass. (*c*) Vaporized I_2 molecules soon spread throughout the crystallization well and diffuse into the crystallization droplet. (*d*) After incubation, the crystals are coloured dark brown. (*e*) The HYPER-VIL technique employs an additional small droplet (∼1.0 µl) of 30% H_2O_2 hydrogen peroxide placed onto a crystallization bridge enclosed in the crystallization well. The droplet of hydrogen peroxide should be introduced into the crystallization well after the colouration of the target crystals by the application of VIL, or the hydrogen peroxide will redissolve I_2 molecules in the iodine droplet, which would decrease the amount of I_2 vapour diffusion. (*f*) As a result of the HYPER-VIL reaction, generation of oxygen bubbles and bleaching of the brown colour are observed in the crystallization droplet, which are good indicators of iodination.

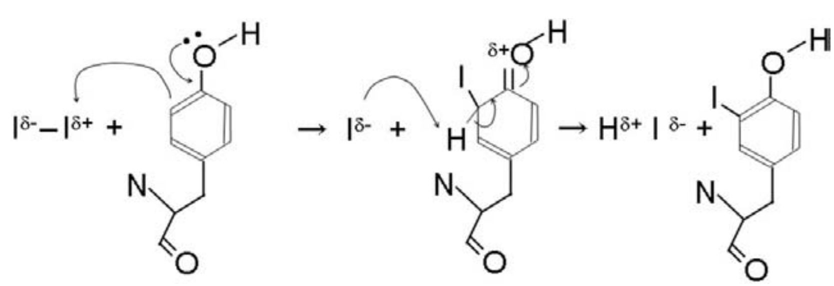

Figure 2
Aromatic electrophilic substitution of iodine involved in the VIL method. A vaporized I_2 molecule diffuses into the crystallization droplet, where the I_2 molecule is polarized, making one end electrophilic ($I^{\delta+}$) and the other nucleophilic ($I^{\delta-}$). The electrophilic end ($I^{\delta+}$) then attacks the *ortho* position of tyrosine and the iodine covalently binds to it.

Table 2
SAD data-collection conditions and statistics.

Values in parentheses are for the outer resolution shell.

	Thaumatin		Lysozyme
Phasing method	SAD	SAD	SAD
Iodine-labelling method/time/temperature	VIL/0.5 h/293 K	VIL/0.5 h/293 K + HYPER-VIL (without iodine droplet)/0.5 h/293 K	VIL/3 d/293 K + HYPER-VIL/3 h/303 K
Wavelength (Å)	2.2908	1.5418	1.5418
Generator, X-ray power (kW)	FR-E, 1.52	RU-300, 4.0	RU-300, 4.0
Detector and optics	R-AXIS VII, Osmic Cr CMF	R-AXIS IV^{++}, Osmic Cu CMF	R-AXIS IV^{++}, Osmic Cu CMF
Camera distance (mm)	115	150	150
Temperature (K)	90	90	90
Exposure time per frame (min)	1.0	5.0	1.0
$\Delta\varphi$ (°)	0.5	1.0	1.0
No. of frames	720	360	360
Rotation angle (°)	360	360	360
Space group	$P4_12_12$	$P4_12_12$	$P4_32_12$
Unit-cell parameters (Å)	$a = b = 57.14$, $c = 151.90$	$a = b = 57.73$, $c = 150.96$	$a = b = 79.70$, $c = 36.12$
Resolution (Å)	50.00–2.38 (2.46–2.38)	50.00–2.30 (2.38–2.30)	50.00–2.1 (2.18–2.10)
Mosaicity (°)	0.24	0.54	0.47
$B_{\rm Wilson}$ (Å^2)	40.9	34.4	28.1
Total reflections	199109	321917	153757
Unique reflections (Friedel pairs unmerged)	17447	21684	12996
$R_{\rm merge}$ (%)	0.080 (0.146)	0.092 (0.256)	0.075 (0.199)
Completeness (%)	90.4 (32.6)	100.0 (100.0)	99.8 (99.9)
Redundancy	11.4 (2.5)	14.8 (14.8)	11.8 (9.2)
$I/\sigma(I)$	67.8 (11.4)	61.1 (16.9)	66.7 (10.3)
$\langle\lvert\Delta F_{\rm ano}\rvert/F\rangle$ (%)	8.87	7.04	3.60

Table 3
SIRAS/MIRAS data-collection conditions and statistics.

Values in parentheses are for the outer resolution shell.

	Trypsin		Xylanase		
Phasing method	SIRAS			MIRAS	
Iodine-labelling method/time/temperature	Native	VIL/20 h/303 K + HYPER-VIL/18.5 h/303 K	Native	VIL/7 d/293 K	VIL/7 d/293 K + VIL/0.5 d/303 K
Wavelength (Å)	1.5418	1.5418	1.5418	1.5418	1.5418
Generator, X-ray power (kW)	RU-300, 4.0	FR-E, 2.025	RU-300, 4.0	FR-E, 2.025	FR-E, 2.025
Detector and optics	R-AXIS IV^{++}, Osmic Cu CMF	R-AXIS IV, Osmic Cu CMF	R-AXIS IV^{++}, Osmic Cu CMF	R-AXIS IV, Osmic Cu CMF	R-AXIS IV, Osmic Cu CMF
Camera distance (mm)	150	150	150	150	150
Temperature (K)	90	90	90	90	90
Exposure time per frame (min)	1.0	1.0	8.0	1.0	1.0
$\Delta\varphi$ (°)	1.0	1.0	1.0	1.0	1.0
No. of frames	180	360	360	360	360
Rotation angle (°)	180	360	360	360	360
Space group	$P2_12_12_1$	$P2_12_12_1$	$P2_1$	$P2_1$	$P2_1$
Unit-cell parameters (Å, °)	$a = 54.227$, $b = 57.927$, $c = 66.829$	$a = 54.323$, $b = 58.197$, $c = 66.620$	$a = 40.15$, $b = 38.53$, $c = 56.73$, $\beta = 110.33$	$a = 40.30$, $b = 38.59$, $c = 57.15$, $\beta = 110.29$	$a = 40.19$, $b = 38.56$, $c = 56.79$, $\beta = 110.18$
Resolution (Å)	50–2.01 (2.08–2.01)	50–2.00 (2.07–2.00)	50–2.00 (2.07–2.00)	50–2.01 (2.08–2.01)	50–2.00 (2.07–2.00)
Mosaicity (°)	0.35	0.33	1.0	0.36	1.1
$B_{\rm Wilson}$ (Å^2)	16.3	23.5	24.2	21.8	26.0
Total reflections	102464	175119	56266	59009	51285
Unique reflections (Friedel pairs unmerged)	27087	27541	19192	20743	18789
$R_{\rm merge}$(%)	0.081 (0.226)	0.073 (0.168)	0.069 (0.147)	0.066 (0.142)	0.052 (0.171)
Completeness (%)	100 (99.9)	99.8 (99.6)	89.0 (78.8)	96.4 (91.8)	87.1 (71.3)
Redundancy	3.8 (3.7)	6.4 (5.6)	2.9 (2.4)	2.8 (2.4)	2.7 (1.9)
$I/\sigma(I)$	44.2 (0.98)	6.4 (1.6)	6.3 (1.2)	4.9 (1.1)	27.6 (4.3)
$\langle\lvert\Delta F_{\rm ano}\rvert/F\rangle$ (%)	—	4.32	—	5.47	6.32

To increase the degree of iodination in thaumatin, the hydrogen peroxide vaporizing iodine labelling (HYPER-VIL) technique was subsequently applied to the crystals at 293 K (Figs. 1*e* and 1*f*). After the removal of the iodine droplet from the cover glass, a small droplet (1 µl) of hydrogen peroxide (H_2O_2) was incorporated into the crystallization well for 0.5 h (Fig. 1*e*). Soon after the resealing of the crystallization well with the cover glass, H_2O_2 vapour diffused into the droplet, enhancing the iodination reaction. During the procedure, oxygen (O_2) bubbles were observed in the droplet (Fig. 1*f*).

Other iodination of test crystals by VIL or HYPER-VIL was performed using similar procedures to those above, using different incubation times and temperatures (Tables 2 and 3). Crystals of glucose isomerase disintegrated so rapidly on application of VIL, even when using smaller KI/I_2 droplets, that we could not prepare useful iodinated derivatives.

2.4. Data collection and structural analysis

Diffraction data were collected from the iodinated crystals using in-house Cu $K\alpha$ X-ray systems consisting of an RU-300 X-ray generator, an R-AXIS IV^{++} imaging-plate detector and confocal Cu mirror optics or an FR-E super-brilliant X-ray generator, R-AXIS IV imaging-plate detector and confocal Cu mirror optics (all from Rigaku/MSC, Tokyo, Japan). Cr $K\alpha$ X-ray data were collected using a system consisting of an FR-E super-brilliant X-ray generator, an R-AXIS VII imaging-plate detector and confocal Cr mirror optics (Rigaku/MSC). All diffraction data were integrated and scaled with the program *HKL*2000 (Otwinowski & Minor, 1997). We used all diffraction data for the phase calculations without any resolution cutoff, because in all cases the best results for the phasing were obtained with full data sets, even if the completeness or $I/\sigma(I)$ for the outer shells were low. The initial iodinated sites were determined using the program *SOLVE* (Terwilliger & Berendzen, 1999). Further phase determination was carried out using the program *autoSHARP* (Bricogne *et al.*, 2003) and subsequent density modification was performed using the program *SOLOMON* (Abrahams & Leslie, 1996). The initial models automatically built using the programs *ARP*/*wARP* (Perrakis *et al.*, 1999) or *RESOLVE* (Terwilliger & Berendzen, 1999) were manually modified using the program *XtalView* (McRee, 1999). These structures were refined using the program *CNS* (Brünger *et al.*, 1998), involving the anomalous scattering effects of Cr $K\alpha$ ($f' = -5.85$, $f'' = 12.83$) or Cu $K\alpha$ ($f' = -0.59$, $f'' = 6.84$).

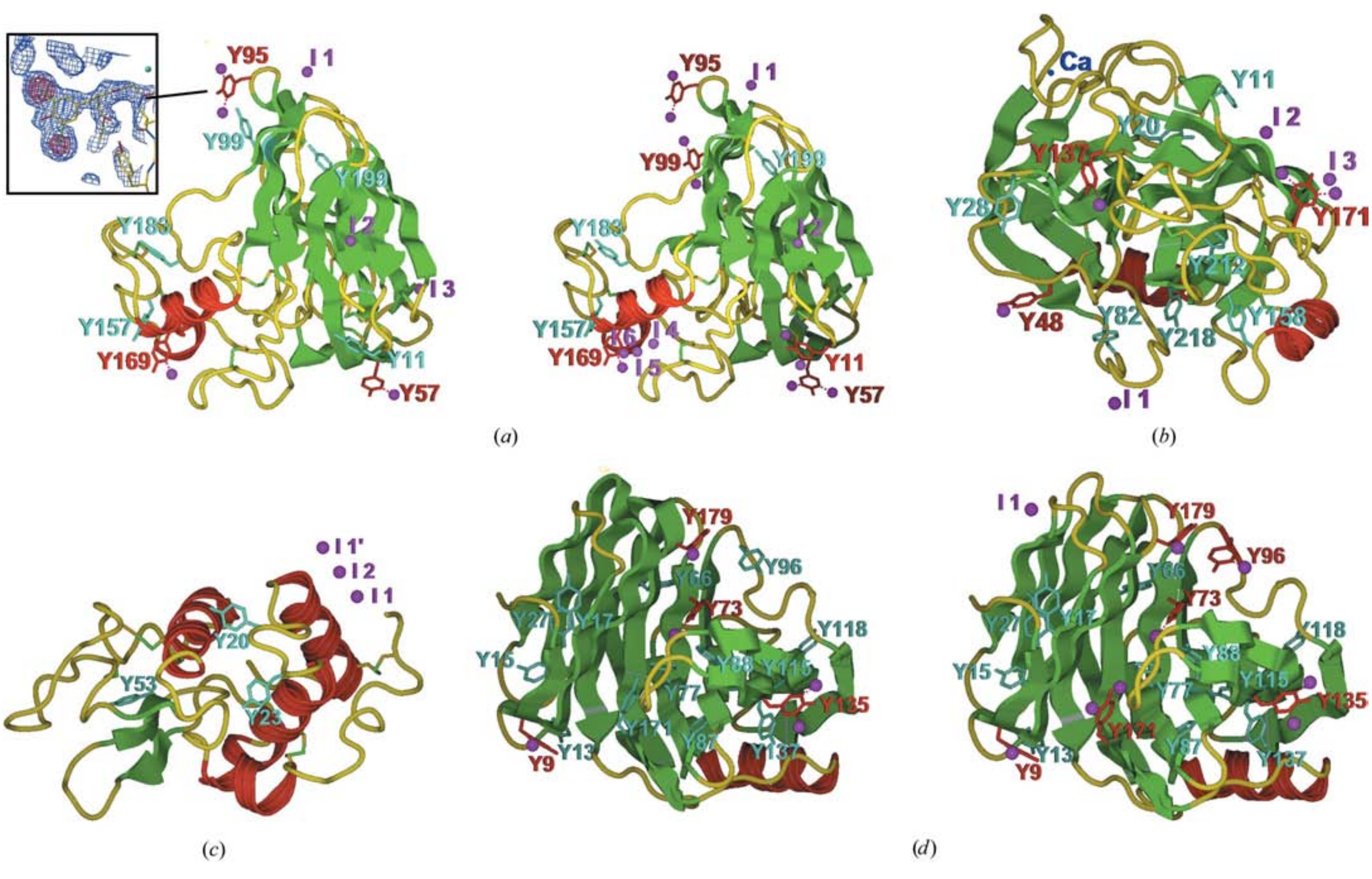

Figure 3
Schematic drawings of iodinated proteins prepared by VIL and HYPER-VIL (depicted using the program *NOC*; http://noc.ibp.ac.cn; the close-up picture of Tyr95 with the electron-density maps in VIL-thaumatin was drawn using the program *XtalView*). In the molecular pictures, iodinated tyrosines are coloured red, I atoms are in purple and tyrosines that are not involved in iodination are drawn in cyan. (*a*) Left, VIL-thaumatin with a close-up picture showing around iodinated tyrosine Tyr95 superposed in the I-SAD phased electron-density maps (red > 5σ, blue > 1σ); right, HYPER-VIL-thaumatin. (*b*) HYPER-VIL-trypsin. (*c*) HYPER-VIL-lysozyme prepared by the HYPER-VIL technique. Iodide I2 is on a special position. (*d*) Left, VIL-xylanase; right, VIL′-xylanase.

Table 4
Automatic phasing and model-building statistics.

Protein (No. of residues)	Thaumatin (207)		Trypsin (219)	Lysozyme (129)	Xylanase (176)
Iodine-labelling method	VIL	HYPER-VIL	HYPER-VIL	HYPER-VIL	VIL
Phasing method	SAD	SAD	SIRAS	SAD	MIRAS
Resolution (Å)	50–2.38	50–2.30	50–2.0	50–2.1	50–2.0
SHARP FOM (acentric/centric)	0.561/0.175	0.535/0.213	0.51/0.43	0.362/0.105	0.376/0.313
After *SOLOMON*	0.841	0.954	0.885	0.807	0.798
ARP/*wARP* building (side chains built)	206 (158)	204 (204)	219 (219)	—	—
RESOLVE building (side chains built)	—	—	—	86 (47)	124 (16)

Table 5
Refinement and iodine-binding statistics of VIL-thaumatin and HYPER-VIL-thaumatin.

(*a*) Refinement using *CNS*.

Iodine-labelling method	VIL	HYPER-VIL
Resolution (Å)	40.41–2.38	31.7–2.30
$R_{\rm work}/R_{\rm free}$ (%)	23.1/26.2	21.4/25.0
R.m.s.d. in bond lengths (Å)	0.008	0.007
R.m.s.d. in bond angles (°)	1.5	1.4
No. of waters	54	36

(*b*) I—C distances and occupancies for iodotyrosines.

Iodine-labelling method	VIL						HYPER-VIL					
	I1			I2			I1			I2		
Iodotyrosine	$I1—C^{\varepsilon1}$ (Å)	Occupancy	B (Å^2)	$I2—C^{\varepsilon2}$ (Å)	Occupancy	B (Å^2)	$I1—C^{\varepsilon1}$ (Å)	Occupancy	B (Å^2)	$I2—C^{\varepsilon2}$ (Å)	Occupancy	B (Å^2)
Tyr11	—	—	—	—	—	—	2.09	0.82	32.4	2.09	0.79	38.3
Tyr57	2.09	0.88	23.9	—	—	—	2.07	1.00	32.2	2.08	0.81	32.5
Tyr95	2.09	0.59	31.5	2.09	0.81	25.8	2.11	0.72	41.3	2.10	0.99	41.1
Tyr99	—	—	—	—	—	—	2.11	0.71	41.5	2.10	0.67	44.7
Tyr169	2.08	0.22	17.7	—	—	—	2.11	0.97	27.3	—	—	—

(*c*) Occupancies and interactions of iodide ions. Residues from symmetry-related molecule are marked with asterisks. I4–I6 make a triiodide with distances I4—I5 of 3.36 Å, I5—I6 of 3.09 Å and an angle I4—I5—I6 of 163.3°.

Iodine-labelling method	VIL			HYPER-VIL		
Iodide ion (I^-)	Occupancy	B (Å^2)	Interaction (corresponding residues)	Occupancy	B (Å^2)	Interaction (corresponding residues)
I1	0.73	32.1	Hydrophobic (Gly96, Gly195, *Pro135)	0.30	48.9	Hydrogen bond (Asn93 OD1), hydrophobic (*Pro135)
I2	0.55	49.3	Hydrophobic (*Lys163), hydrogen bond (Arg125 NH2, Arg8 NH1)	0.64	48.2	Hydrogen bond (Arg125 NH2)
I3	0.33	30.4	Hydrophobic (Arg25, Leu75)	—	—	—
I4	—	—	—	0.65	45.3	Hydrogen bond (Arg175 NH1), hydrophobic (Arg175, *Gly44)
I5	—	—	—	0.48	40.3	Hydrogen bond (Wat12)
I6	—	—	—	0.58	44.4	Hydrogen bond (Glu168), hydrophobic (Pro135, I1-Tyr169)

3. Results

Data-collection statistics are summarized in Tables 2 and 3. Data collection using Cr $K\alpha$ X-rays (λ = 2.2908 Å) was only available for the iodinated thaumatin prepared by VIL (VIL-thaumatin), while the data for HYPER-VIL-thaumatin, HYPER-VIL-trypsin, HYPER-VIL-lysozyme, VIL-xylanase and VIL′-xylanase (extra iodine stock solution applied and extended incubation time with higher temperature) were collected using Cu $K\alpha$ X-rays (λ = 1.5418 Å). Statistics for automatic phasing and model building are summarized in Table 4. Iodide ions bind to each protein by hydrogen-bonding or hydrophobic interactions, which are summarized in Tables 5, 6, 7 and 8. Refinement statistics of those proteins including iodine-site information are shown in Tables 5, 6, 7 and 8.

3.1. VIL- and HYPER-VIL-thaumatin

The structure of VIL-thaumatin was automatically built with 206 residues (158 side chains were built) by the program *ARP*/*wARP* (Perrakis *et al.*, 1999) into the electron-density map phased by I-SAD, where Tyr57 and Tyr169 were singly

Table 6
Refinement and iodine-binding statistics of HYPER-VIL-trypsin.

(*a*) Refinement using *CNS*.

Iodine-labelling method	HYPER-VIL
Resolution (Å)	33.3–2.00
$R_{\rm work}/R_{\rm free}$(%)	23.1/26.8
R.m.s.d. in bond lengths (Å)	0.007
R.m.s.d. in bond angles (°)	1.4
No. of waters	93
No. of Ca atoms	1

(*b*) I—C distances and occupancies for iodotyrosines.

Iodine-labelling method	HYPER-VIL					
	I1			I2		
Iodotyrosine	I1—C$^{\varepsilon 1}$ (Å)	Occupancy	B (Å^2)	I2—C$^{\varepsilon 2}$ (Å)	Occupancy	B (Å^2)
Tyr48	2.12	0.42	30.6	—	—	—
Tyr137	2.08	0.59	51.0	—	—	—
Tyr171	2.09	1.00	33.4	2.12	0.67	41.8

(*c*) Occupancies and interactions of iodide ions. Residues from symmetry-related molecule are marked with asterisks.

Iodine-labelling method	HYPER-VIL		
Iodide ion (I$^-$)	Occupancy	B (Å^2)	Interaction (corresponding residues)
I1	0.46	55.3	Hydrogen bond (Ser81 OG, *Gln53 NE2)
I2	0.56	42.8	Hydrogen bond (Gln121 NE2)
I3	0.62	76.7	Hydrophobic (I2-Tyr171)

Table 7
Refinement and iodine-binding statistics of HYPER-VIL-lysozyme.

(*a*) Refinement with *CNS*.

Iodine-labelling method	HYPER-VIL
Resolution (Å)	19.9–2.10
$R_{\rm work}/R_{\rm free}$ (%)	25.2/29.0
R.m.s.d. in bond lengths (Å)	0.005
R.m.s.d. in bond angles (°)	1.3
No. of waters	57

(*b*) Occupancies and interactions of iodide ions. Residues from a symmetry-related molecule are marked with asterisks.

Iodine-labelling method	HYPER-VIL		
Iodide ion (I$^-$)	Occupancy	B (Å^2)	Interaction (corresponding residues)
I1	0.82	49.2	Hydrogen bond (Arg128), hydrophobic (Ala10)
I2 (on a special position)	0.50	31.6	Hydrophobic (Arg14, *Arg14)

iodinated and Tyr95 was doubly iodinated (VIL-thaumatin in Fig. 3*a*). Three iodide ions (I1–I3) were bound to the molecular surface by hydrogen bonds and hydrophobic interactions (Table 5).

On the other hand, iodination in HYPER-VIL-thaumatin was significantly enhanced, with additional iodination sites and generally higher occupancies; all tyrosine residues Tyr11, Tyr57, Tyr95 and Tyr99 were doubly iodinated, except for the singly iodinated Tyr169 (HYPER-VIL-thaumatin in Fig. 3*a*). In addition, five iodide ions (I1–I2, I4–I6) were bound to the molecular surface (Table 5), where I4–I6 was a triiodide. The resultant greater phasing power of HYPER-VIL-thaumatin enabled the program *ARP*/*wARP* to build a total of 204 residues of thaumatin with all side chains built (Table 2), even using Cu $K\alpha$ X-rays instead of Cr $K\alpha$. This result clearly shows that hydrogen peroxide can promote the VIL reaction if the crystalline order of target crystals is resistant to exposure to hydrogen peroxide.

3.2. HYPER-VIL-trypsin

Trypsin (219 residues) was not iodinated by VIL even after 20 h incubation at 303 K (data not shown). Thus, for the purpose of enhancing the iodination, the HYPER-VIL technique was subsequently applied to the trypsin crystals at 303 K. As a result, Tyr48 and Tyr137 were singly iodinated and Tyr171 was doubly iodinated (Fig. 3*b*). Two iodide ions (I1–I2) were bound to the molecular surface by hydrogen bonds and hydrophobic interactions (Table 6). However, SAD phasing of the iodinated trypsin with Cu $K\alpha$ X-rays failed owing to the lower phasing power (<1.0). The reason for the failure of the SAD phasing might be related to the relatively lower redundancy of a SAD data set or poorer overall $I/\sigma(I)$ compared with other SAD data sets. Thus, instead of the SAD phasing, SIRAS phasing using additional diffraction data from native trypsin (Table 3) provided sufficient phasing power to build a total of 219 residues with all side chains built (Table 4). This result shows that the VIL and HYPER-VIL techniques can prepare isomorphous derivatives that are also suitable for SIRAS or MIRAS phase determinations.

3.3. HYPER-VIL-lysozyme

Crystals of lysozyme were not iodinated by the VIL technique. The subsequent HYPER-VIL approach dissolved the crystals in 6 h; therefore, the HYPER-VIL application was limited to 3 h. Consequently, the tyrosine residues were still not iodinated, perhaps because the accessibility of I_2 molecules to the tyrosines on the molecular surface was limited in the tetragonal crystal packing. Instead, two I atoms (I1–I2) were bound to the molecular surface (Fig. 3*c*). One of the iodide ions (I2) was on a special position. Because the unit-cell parameters of the iodinated lysozyme ($P4_32_12$, $a = b = 79.7$, $c = 36.1$ Å) differed from those of the native crystal ($P4_32_12$, $a = b = 77.8$, $c = 37.3$ Å), only SAD phasing (Table 2) using the HYPER-VIL-lysozyme was successful in obtaining an interpretable electron-density map, in which 86 resides were automatically built (Table 4). Evans & Bricogne (2002) reported the structure of KI/I_2-soaked lysozyme (PDB code 1gwd), in which IOD1130 and IOD1147 (on a special position) are in positions corresponding to I1 and I2 (on a special position) of HYPER-VIL-lysozyme, respectively. The distance between IOD1130 and IOD1147 is 2.72 Å, while that between I1 and I2 is 3.46 Å. In the soaked lysozyme, IOD1130 and

Table 8
Refinement and iodine-binding statistics of VIL-xylanase and VIL′-xylanase.

(*a*) Refinement with *CNS*.

Iodine-labelling method	VIL	VIL′ (extra KI/I_2 added)
Resolution (Å)	18.98–2.01	20.1–2.00
R_{work}/R_{free} (%)	19.8/22.8	20.9/25.3
R.m.s.d. in bond lengths (Å)	0.007	0.008
R.m.sd. in bond angles (°)	1.4	1.4
No. of waters	111	52

(*b*) I—C distances and occupancies for iodotyrosines.

Iodine-labelling method	VIL						VIL′ (extra KI/I_2 added)					
	I1			I2			I1			I2		
Iodotyrosine	I1—$C^{\varepsilon1}$ (Å)	Occupancy	B (Å^2)	I2—$C^{\varepsilon2}$ (Å)	Occupancy	B (Å^2)	I1—$C^{\varepsilon1}$ (Å)	Occupancy	B (Å^2)	I2—$C^{\varepsilon2}$ (Å)	Occupancy	B (Å^2)
Tyr9	2.10	0.24	34.1	—	—	—	2.11	0.24	36.6	—	—	—
Tyr73	2.11	0.29	38.8	—	—	—	2.10	0.44	35.2	—	—	—
Tyr96	—	—	—	—	—	—	2.09	0.56	55.2	—	—	—
Tyr135	2.10	0.75	42.3	2.09	0.35	48.3	2.09	0.85	45.2	2.09	0.44	49.0
Tyr171	—	—	—	—	—	—	2.07	0.45	47.7	2.12	0.37	46.4
Tyr179	2.09	0.52	40.2	—	—	—	2.11	0.56	37.9	—	—	—

(*c*) Occupancies and interactions of iodide ions.

Iodine-labelling method	VIL			VIL′ (extra KI/I_2 added)		
Iodide ion (I^-)	Occupancy	B (Å^2)	Interaction (corresponding residues)	Occupancy	B (Å^2)	Interaction (corresponding residues)
I1	—	—	—	0.67	51.3	Hydrogen bond (Thr26 OG1), hydrophobic (Gly24, Val25, Asn38)

IOD1147 have occupancies of 0.36 and 0.23, respectively, while those of I1 and I2 are 0.82 and 0.5, respectively (Table 7). This result corresponds with the observation that both VIL and HYPER-VIL can prepare iodothaumatin with generally higher occupancies compared with that prepared by conventional soaking techniques (Zwart *et al.*, 2004). This result also demonstrates that the techniques presented can prepare useful iodinated crystals even if there are no susceptible tyrosine residues in the target proteins.

3.4. Iodination of xylanase by VIL and MIRAS phasing using Cu *Kα* X-rays

The VIL technique was first applied to crystals of xylanase (176 residues) for an incubation time of a week at 293 K. The iodinated xylanase contained singly iodinated tyrosines Tyr9, Tyr73 and Tyr179 and doubly iodinated tyrosine Tyr135 (VIL-xylanase in Fig. 3*d*). The resultant iodinated xylanase crystals, however, generated insufficient phasing power to build an initial model, even by a SIRAS calculation using native and VIL-xylanase. Hydrogen peroxide increased the perturbation of the crystalline order and thus the HYPER-VIL technique could not be used in this case. Therefore, we attempted a further VIL reaction in which an additional fresh droplet of 2 µl KI/I_2 solution was enclosed within the same crystallization well for 12 h at 303 K. This procedure yielded another iodinated crystal of xylanase in which Tyr9, Tyr73, Tyr96 and Tyr179 were singly iodinated and Tyr135 and Tyr171 were doubly iodinated (Table 8). One iodide ion (I1) was bound to the molecular surface. This result shows that extra addition of KI/I_2 stock solution to the crystallization well during the VIL incubation can increase the iodination of the target crystals. Subsequent MIRAS phasing was carried out using the native data coupled with the iodinated derivative data obtained using Cu *Kα* X-rays (Table 3), which in turn generated an interpretable electron-density map with an automatically built initial model of 124 residues (Table 4).

4. Discussion

4.1. Aromatic electrophilic substitution involved in VIL

We should note that the brownish colouration of the target crystals under the VIL application does not assure the preparation of effective derivatives. There were in fact no well ordered I atoms in the dark brown-coloured trypsin crystals prepared by VIL (data not shown), in which I_2 molecules may be disordered in the bulk solvent. In the proposed techniques, subsequent iodination of tyrosine residues or binding of iodide ions to the molecular surfaces of proteins are significant processes for the production of effective iodine derivatives. Such iodination by VIL may occur according to the reaction referred to as aromatic electrophilic substitution, in which diffused I_2 molecules in the target droplet electrophilically substitute the *ortho* position of tyrosine (Fig. 2). Because the electron density at the *ortho* position of tyrosine is strengthened when a hydroxyl proton dissociates from the hydroxyl group of tyrosine, the VIL reaction more readily occurs at the tyrosines in a solution with a pH higher than their pK_a values. However, I_2 will react in basic solution to produce iodate (IO_3^-), which is unreactive with tyrosine. Thus, the iodination of tyrosine depends on many conditions involved in VIL. We should study the pH-dependence of the VIL reaction by further experiments. On the other hand, the hydrogen peroxide involved in HYPER-VIL enhances the concentration of iodide (I^-) according to the chemical reaction

$$I_2 + H_2O_2 \rightarrow 2I^- + 2H^+ + O_2,$$

corresponding to the additional sites (I4–I6) of I^- in HYPER-VIL-thaumatin (Fig. 3*a*). The generation of O_2 bubbles and the bleaching of the blown colour in the target droplets are good indicators of this reaction. In addition, as shown in the test crystals of thaumatin and trypsin, hydrogen peroxide also enhances the iodination of tyrosine. Thus, when enhanced phasing power is required and the target crystals are resistant to hydrogen peroxide, HYPER-VIL may be applied as the first extended choice after the initial VIL approach.

4.2. Dominant experimental conditions responsible for the VIL and HYPER-VIL reactions

The reaction temperatures during VIL or HYPER-VIL were found to be significant experimental factors in controlling the reactions. In the VIL and HYPER-VIL reactions, thaumatin was easily iodinated at 293 K. In contrast, the iodination reactions of trypsin and lysozyme did not occur at 293 K, but did proceed at 303 K. When we increase the temperature of the VIL or HYPER-VIL reactions, aromatic electrophilic substitutions are more likely to occur according to the kinetic theory of chemical reactions. In addition, the partial vapour pressure of iodine is 62.6 Pa at 303 K and 137.3 Pa at 313 K (Matsuoka, 1974). Thus, the amount of vaporized iodine increases with rising temperature, which leads to increasing iodination of the target crystals. The incubation time of VIL or HYPER-VIL is also important in the iodine derivatization. In the case of thaumatin, incubation times of 0.5–1.0 h were sufficient for the derivatization. On the other hand, the crystals of trypsin, xylanase and lysozyme required a longer amount of time for iodine labelling.

4.3. Advantages of the VIL and HYPER-VIL techniques

We will discuss the advantages of the VIL and HYPER-VIL techniques by comparing iodinated thaumatin derivatives prepared by these methods with those prepared by conventional methods. In a previous report, tyrosine residues in thaumatin were iodinated by soaking the crystals in *N*-iodosuccinimide or by mixing the protein solution with the iodizing solution prior to crystallization (Zwart *et al.*, 2004). In those experiments, iodinated crystals grown from the protein/*N*-iodosuccinimide mixture diffracted 1.54 Å X-rays from an NSLS beamline X9B to 2.0 Å resolution. On the other hand, crystals soaked in the 25% saturated *N*-iodosuccinimide solution for 20 min only diffracted X-rays to 2.5 Å resolution. In addition, the mosaicity of these crystals increased from 0.23 to 1.1°. These results suggest that the crystalline order of the soaked thaumatin was damaged, most likely owing to the resultant differences in ionic strength between the native crystals and the iodine-compound solution. Such differences in ionic strength often cause problems in soaking derivatives. In VIL and HYPER-VIL, this problem is subtle because only gaseous iodine and hydrogen peroxide molecules gradually diffuse into the target crystallization droplets from the droplets containing iodine and/or hydrogen peroxide, balancing the vapour pressures between these droplets. HYPER-VIL-thaumatin diffracted in-house X-rays beyond 2.3 Å resolution with a lower mosaicity and Wilson *B* factor (Table 2) compared with those of the soaked thaumatin (Zwart *et al.*, 2004). Moreover, the use of the VIL and HYPER-VIL techniques eliminated the dissolution of iodine compounds into crystallization solution, which often causes problems in conventional heavy-atom soakings owing to low solubility of the compounds.

Owing to the advantages of VIL and HYPER-VIL mentioned above, crystals of trypsin and xylanase were successfully iodinated at the tyrosines, although I-SAD phasing using the derivatives did not generate sufficient phasing power for automatic structure determination when in-house Cu $K\alpha$ X-rays were employed. However, it may be possible to determine the phases of iodinated trypsin or xylanase solely by I-SAD phasing when the occupancies of iodine in the crystals are increased by longer or higher temperature applications of VIL and HYPER-VIL or by using Cr $K\alpha$ X-rays.

4.4. Limitations of the VIL and HYPER-VIL techniques

In the present experiment, the tyrosine residues in lysozyme were not iodinated even using the HYPER-VIL technique. This may be partly because the accessibility of the I_2 molecule to Tyr20, Tyr23 and Tyr53 of lysozyme in the tetragonal crystal packing is more limited compared with that of other smaller molecules or ions such as water molecules or chloride ions. Thus, target crystals that contain only a few tyrosines in I_2-accessible positions result in a lower chance of the iodination of tyrosines. Moreover, degradation of the crystals of glucose isomerase was observed during the VIL procedures, possibly because the packing of molecules in the crystals was affected by the permeation of iodine molecules. Such crystals showing high receptivity to iodination may also be unsuitable for the VIL or HYPER-VIL applications.

5. Conclusions

In this experiment, we were able to iodinate four of the five test crystals using the present VIL or HYPER-VIL techniques, resulting in crystals applicable to SAD, SIRAS and MIRAS phase determinations using Cr $K\alpha$ or Cu $K\alpha$ X-rays. The VIL and HYPER-VIL methods are somewhat similar to the Xe or Kr derivatizations in their use of gaseous diffusion, but the former have several important advantages, such as the fact that they require no pressurization chamber and can make iodine bind irreversibly with target proteins. When useful heavy-atom derivatives cannot be prepared by any conventional method, the VIL and HYPER-VIL techniques may be considered.

We would like to thank Dr Kunio Miki for giving us an opportunity to carry out the current work. We express our gratitude to Dr Noritake Yasuoka for his detailed criticism of the manuscript. We would like to thank Dr Raita Hirose for preparing the thaumatin crystals. We also thank Dr Yasushi Nitanai for helping with the operation of the FR-E Cu $K\alpha$ generator, Professor Isao Tanaka and Dr Nobuhisa Watanabe for their help in the collection of the in-house Cr $K\alpha$ X-ray diffraction data, and Drs Yukihide Kousumi and Hiroshi Kamitakahara for their discussions of the iodination reactions.

References

Abrahams, J. P. & Leslie, A. G. W. (1996). *Acta Cryst.* D**52**, 30–42.

Bricogne, G., Vonrhein, C., Flensburg, C., Schiltz, M. & Paciorek, W. (2003). *Acta Cryst.* D**59**, 2023–2030.

Brünger, A. T., Adams, P. D., Clore, G. M., DeLano, W. L., Gros, P., Gross-Kunstleve, R. W., Jiang, J.-S., Kuszewski, J., Nilges, M., Pannu, N. S., Read, R. J., Rice, L. M., Simonson, T. & Warren, G. L. (1998). *Acta Cryst.* D**54**, 905–921.

Brzozowski, A. M., Derewenda, U., Derewenda, Z. S., Dodson, G. G., Lawson, D. M., Turkenburg, J. P., Bjorkling, F., Huge-Jensen, B., Patkar, S. A. & Thim, L. (1991). *Nature (London)*, **351**, 491–494.

Chayen, N. E., Cianci, M., Olczak, A., Raftery, J., Rizkallah, P. J., Zagalsky, P. F. & Helliwell, J. R. (2000). *Acta Cryst.* D**56**, 1064–1066.

Cohen, A., Ellis, P., Kresge, N. & Soltis, M. (2001). *Acta Cryst.* D**57**, 233–238.

Dauter, Z. (2002). *Curr. Opin. Struct. Biol.* **12**, 674–678.

Dauter, Z., Dauter, M., de La Fortelle, E., Bricogne, G. & Sheldrick, G. M. (1999). *J. Mol. Biol.* **289**, 83–92.

Dauter, Z., Dauter, M. & Rajashankar, K. R. (2000). *Acta Cryst.* D**56**, 232–237.

Evans, G. & Bricogne, G. (2002). *Acta Cryst.* D**58**, 976–991.

Evans, G. & Bricogne, G. (2003). *Acta Cryst.* D**59**, 1923–1929.

Ghosh, D., Erman, M., Sawicki, M., Lala, P., Weeks, D. R., Li, N., Pangborn, W., Thiel, D. J., Jornvall, H., Gutierrez, R. & Eyzaguirre, J. (1999). *Acta Cryst.* D**55**, 779–784.

Hendrickson, W. A. (1991). *Science*, **254**, 51–58.

Kitago, Y., Watanabe, N. & Tanaka, N. (2005). *Acta Cryst.* D**61**, 1013–1021.

Leinala, E. K., Davies, P. L. & Jia, Z. (2002). *Acta Cryst.* D**58**, 1081–1083.

Liu, Z. J., Vysotski, E. S., Chen, C. J., Rose, J. P., Lee, J. & Wang, B.-C. (2000). *Protein Sci.* **9**, 2085–2093.

McRee, D. E. (1999). *J. Struct. Biol.* **125**, 156–165.

Matsuoka, K. (1974). *Review of Iodine*, p. 36. Tokyo: Kasumigaseki Shuppan.

Mueller-Dieckmann, C., Polentarutti, M., Djinovic, C. K., Panjikar, S., Tucker, P. A. & Weiss, M. S. (2004). *Acta Cryst.* D**60**, 28–38.

Nagem, R. A. P., Ambrosio, A. L. B., Rojas, A. L., Navarro, M. V. A. S. Golubev, A. M., Garratt, R. C. & Polikarpov, I. (2005). *Acta Cryst.* D**61**, 1022–1030.

Nagem, R. A. P., Dauter, Z. & Polikarpov, I. (2001). *Acta Cryst.* D**57**, 996–1002.

Olczak, A., Cianci, M., Hao, Q., Rizkallah, P. J., Raftery, J. & Helliwell, J. R. (2003). *Acta Cryst.* A**59**, 327–334.

Otwinowski, Z. & Minor, W. (1997). *Methods Enzymol.* **276**, 307–326.

Owen, D. J. & Evans, P. R. (1998). *Science*, **282**, 1327–1332.

Perrakis, A., Morris, R. M. & Lamzin, V. S. (1999). *Nature Struct. Biol.* **6**, 458–463.

Sauer, O., Schmidt, A. & Kratky, C. (1997). *J. Appl. Cryst.* **30**, 476–486.

Schiltz, M., Prangé, T. & Fourme, R. (1994). *J. Appl. Cryst.* **27**, 950–960.

Soltis, S. M., Stowell, M. H. B., Wiener, M. C., Phillips, G. N. & Rees, D. C. (1997). *J. Appl. Cryst.* **30**, 190–194.

Stowell, M. H. B., Soltis, S. M., Kisker, C., Peters, J. W., Schindelin, H., Rees, D. C., Cascio, D., Beamer, L., Hart, P. J., Wiener, M. C. & Whitby, F. G. (1996). *J. Appl. Cryst.* **29**, 608–613.

Sigler, P. B. (1970). *Biochemistry*, **9**, 3609–3617.

Takeda, K., Miyatake, H., Park, S. Y., Kawamoto, M., Kamiya, N. & Miki, K. (2004). *J. Appl. Cryst.* **37**, 925–933.

Terwilliger, T. C. & Berendzen, J. (1999). *Acta Cryst.* D**55**, 849–861.

Verdon, G., Albers, S. V., Dijkstra, B. W., Driessen, A. J. M. & Thunnissen, A.-M. W. H. (2002). *Acta Cryst.* D**58**, 362–365.

Xie, J., Wang, L., Wu, N., Brock, A., Spraggon, G. & Schultz, P. (2004). *Nature Biotechnol.* **22**, 1297–1301.

Zwart, P. H., Banumathi, S., Dauter, M. & Dauter, Z. (2004). *Acta Cryst.* D**60**, 1958–1963.